

Spectrophotometric pH measurement in the ocean: Requirements, design, and testing of an autonomous charge-coupled device detector system

Karsten Friis*, Arne Körtzinger, and Douglas W.R. Wallace

Leibniz-Institut für Meereswissenschaften, FB Marine Biogeochemistry, Düsternbrooker Weg 20, D-24105 Kiel, Germany

Abstract

A newly designed system for high quality discrete spectrophotometric measurements of pH_T using a low-cost charge-coupled device (CCD) detector is described. Considerations and requirements for the choice of spectrophotometers with a CCD detector instead of scanning spectrophotometers with photomultiplier detector are elucidated. The presented system is evaluated in the laboratory for system accuracy and short-term precision and at sea for long-term precision and at-sea capability. Derived system characteristics are a (1s) short-term precision of ± 0.0012 pH units and a (1s) long-term precision at sea of ± 0.0032 pH units based on Certified Reference Materials (CRM). Such long-term precision is equivalent to a deviation of ± 1.1 to $2.2 \mu\text{mol kg}^{-1}$ in total dissolved inorganic carbon (TCO_2) and ± 1.4 to $2.1 \mu\text{mol kg}^{-1}$ in total alkalinity (TA), depending on temperature and the TCO_2/TA ratio. Overdetermination of the CO_2 system (TCO_2 , TA, pH_T) from surface-to-deep water profiles support the accuracy and precision assessment in comparison to earlier data. With careful design and testing, low-cost CCD spectrophotometers can be used for high accuracy pH measurements.

pH is a master variable affecting the equilibria and kinetics of a wide range of chemical processes in the ocean. Marine pH is governed by the CO_2 system, which can be explained by a classical buffer concept consisting of carbonate salts and carbonic acid. Four different measurement parameters are available to describe the CO_2 system: the partial pressure of CO_2 ($p\text{CO}_2$), total dissolved inorganic carbon (TCO_2), total alkalinity (TA), and pH. In combination with an adequate thermodynamic model of the seawater, and the knowledge of the dissociation constants of carbonic acid, any combination of two of these CO_2 parameters allows calculation of the other two.

*Current address: Pennsylvania State University, Department of Meteorology, 503 Walker Building, University Park, PA 16802-5013, USA. Telephone 814-863-1036. Fax 814-865-3663. E-mail: kfriis@meteo.psu.edu

Acknowledgments

We thank the captain and crew of the R/V *Meteor* and the chief scientists, W. Zenk and F. Schott, for their cooperation during the research cruises; and L. Mintrop and J.C. Duinker for their helpful comments on an earlier version of this pH system. The manuscript was improved significantly due to the comments of the reviewers A.G. Dickson and R.G.J. Bellerby and the associate editor R.H. Byrne. This is highly appreciated. We also want to thank K.M. Johnson, who did the TCO_2 -analysis and M.D. DeGrandpre, who had a careful look on an earlier version of the manuscript. This work was supported by the *Deutsche Forschungsgemeinschaft* under the SFB 460.

Since the onset of the industrial revolution, pH has decreased in the surface ocean due to an atmospheric $p\text{CO}_2$ increase of more than 30% (i.e., of $\sim 90 \mu\text{atm}$ in 2000) and the resulting CO_2 flux from the atmosphere into the surface ocean. The corresponding acidification is about 0.1 pH units, which is about equal to the seasonal pH change in oligotrophic waters and about a third to a half of that in eutrophic waters, mainly due to biological activity. This is found to have an impact on marine biota, and first reports of decreasing calcification success of corals and planktonic organisms have been given (Buddemeier et al. 1998; Riebesell et al. 2000).

We used spectrophotometric pH measurements from repeated hydrographic surveys to identify and quantify the anthropogenic CO_2 transient in the north Atlantic Ocean. The increase of surface water $p\text{CO}_2$ due to the uptake of atmospheric $p\text{CO}_2$ drives a pH decrease of about 0.002 pH units per year (at constant alkalinity). The required analytical accuracy of seawater pH measurements is therefore of the same order. Spectrophotometric pH data with such accuracy (± 0.005 pH units) and precision (± 0.0004 – 0.001 pH units) have been reported (Clayton and Byrne 1993; McElligott et al. 1998; DelValls 1999; Tapp et al. 2000; Bellerby et al. 2002; Martz et al. 2003). These measurements were performed manually with scanning spectrophotometers featuring photomultiplier detectors (scanning time of about a minute) with photo diode arrays (PDA) and charge-coupled device (CCD) detectors (Tapp et

Table 1. The definitions of hydrogen ion concentrations underlying the pH scales in seawater*

Scale name	Definition
Free	$[H_F] = [H^+]$
Total	$[H_T] = [H_F] (1 + S_T / K(\text{HSO}_4^-)) \approx [H^+] + [\text{HSO}_4^-]$
Seawater	$[H_{\text{SWS}}] = [H_F] (1 + S_T / K(\text{HSO}_4^-) + F_T / K(\text{HF})) \approx [H^+] + [\text{HSO}_4^-] + [\text{HF}]$

* S_T is the total concentration of sulfate ions ($\text{SO}_4^{2-} + \text{HSO}_4^-$), F_T is the total concentration of fluoride ions ($\text{F}^- + \text{HF}$), and $K(\text{HSO}_4^-)$ and $K(\text{HF})$ are the acid dissociation constants HSO_4^- and HF . Because $\text{SO}_4^{2-} > \text{HSO}_4^-$ and $\text{F}^- > \text{HF}$, the scale definitions simplify in very good numerical approximation, as shown also.

al. 2000, Bellerby et al. 2002). The CCD detector systems are significantly cheaper. Additionally, the optics of this new generation of detectors are less sensitive to vibration and, therefore, ideal for seagoing systems. The CCD spectrophotometer design facilitates modular exchanges and hence incessant improvements of existing systems.

Tapp et al. (2000) and Bellerby et al. (2002) used earlier, less sensitive versions of the CCD spectrophotometer that was used here. Their work mainly concentrated on automation aspects, system stability at sea, and performance tests. Nevertheless, an increased potential for a wider distribution of new spectrophotometric pH systems needs clear definitions of analytical requirements and possibilities. Here we present a new automated high precision spectrophotometric pH system, completely describe its design from syringe pump to light filtering, and discuss important requirements, including frequently neglected aspects of accurate marine pH analysis.

pH scales in marine systems—In marine chemistry, pH is usually defined on one of several slightly differing concentration scales:

$$\text{pH}_X = -\lg[H_X^+] \quad (1)$$

where the subscript X is F for the free, T for the total, or SWS for the seawater scale. The formal definitions of these scales are given in Table 1. The differences between these scales reflect differences in the seawater model employed, i.e., in the composition of the artificial seawater used for the pH scale calibration. For example, the “seawater scale” calibration needs artificial or natural seawater containing salts of the conservative and not completely dissociated acids HF and HSO_4^- . The “total” hydrogen scale calibration needs artificial seawater containing only HSO_4^- , and the “free” hydrogen scale calibration needs seawater including only fully dissociated salts. The seawater scale is closest in composition to natural seawater, and the pH definition includes hydrogen associated with fluoride and sulfate. Therefore, errors associated with the dissociation constants for HF and HSO_4^- are avoided. As opposed to the seawater scale, the total scale includes hydrogen associated with sulfate only. The difference between the seawater scale and the total scale is about -0.01 pH units at a salinity of 35. The error avoided by using the seawater scale is about

0.0003 pH units, if one assumes a rather realistic (but not directly reported) error of 3% in the determination of the commonly used acid dissociation constant of HF that is based on measurements of Culberson et al. (1970). With regard to desired accuracy, we chose the total scale (in mol kg^{-1} seawater) for the present work. With this choice, we are in agreement with the majority of the CO_2 community.

Measurements in seawater—Precise measurement of seawater pH can be performed by potentiometric methods with glass electrodes as well as by spectrophotometric methods. The potentiometric measurement has the advantage of requiring relatively small and inexpensive equipment, however, data quality depends strongly on the preparation of seawater calibration buffers, which are frequently a problem. The calibration buffer preparation is error-prone, and the buffers should ideally be checked on shore with an electrochemical cell of platinum/hydrogen electrode versus silver/silver chloride electrode ($\text{Pt}/\text{H}_2//\text{Ag}/\text{AgCl}$). At sea, the buffer stability must be controlled. To overcome such problems, Byrne (1987) proposed to use spectrophotometric methods using pH indicator dyes. Spectrophotometric pH measurements are not prone to the problems associated with buffers. The calibration of indicator solution and measurement system can be done in a shore-based laboratory and the system precision can be tested with any stable batch of seawater. A thermodynamical overview of both methods has been given by Dickson (1993a).

Since 1987, several indicators have been suggested and calibrated for spectrophotometric pH measurements in marine environments (Robert-Baldo et al. 1985; Byrne 1987; Clayton and Byrne 1993; Zhang and Byrne 1996). The optimum pH range for an indicator dye is determined by its pK value, and the extinction coefficient ratios of the basic and acidic indicator forms (DOE 1994). The pH indicator meta-cresol purple has been proposed as optimal for the pH range encountered in typical surface-to-deep water profiles, whereas thymol blue has been proposed for surface water measurements that are within a relatively narrow pH range (Table 2).

Materials and procedure

Spectrophotometric calculation procedure—Spectrophotometric pH determination is based on the absorbance spectra of a pH indicator dye, which has a pK value centered in the expected oceanic pH and colored protonated and deprotonated forms. From the absorbance ratio of the unprotonated and protonated forms (R), the pH can be calculated using Eq. 2 (Robert-Baldo et al. 1985; Clayton and Byrne 1993; DOE 1994; Zhang and Byrne 1996; Wedborg et al. 1999):

$$\text{pH}_X = pK_{\text{ind}} + \lg\left(\frac{R - e_1}{e_2 - R e_3}\right) \quad (2)$$

The e -values are extinction coefficient ratios and are either constants or functions of temperature, which are published together with the pK values for indicators like phenol red

Table 2. pH_T calculation equations of the optional indicators in the presented pH-system ($[H^+]$ in $[mol\ kg^{-1} - SW]$; T in $[K]$)*

Indicator	λ_{HInd}^{max}	λ_{Ind-}^{max}	λ_{iso}	$e_1 \dagger$	$e_2 \ddagger$	$e_3 \P$
mCP	434	578	487.6	0.00691	2.2220	0.1331
TB#	435	596	495	$= -0.00132 + 1.6 \cdot 10^{-5} T$	$= 7.2326 - 0.0299717 T + 4.6 \cdot 10^{-5} T^2$	$= 0.0223 + 0.0003917 T$
PR**	433	558	479.7	0.0038	2.6155	0.1234

Indicator	pK (on the total scale)	Operating range
mCP	$= 1245.69/T + 3.8275 + 0.0021 (35 - S)$	$30 \leq S \leq 37$ $20 \leq T [^\circ C] \leq 30$
TB#	$= 4.706 \text{ second}/T + 26.3300 - 7.17218 \lg T - 0.017316 S$	$30 \leq S \leq 40$ $5 \leq T [^\circ C] \leq 35$
PR**	$= -4054.8374/T + 116.6037 - 38.6645 \lg T + 0.004 (35 - S) - \lg (1 - 0.00106 S)$	$33 \leq S \leq 37$ $0 \leq T [^\circ C] \leq 35$

* $\epsilon_{HInd}^{\lambda_{HInd}^{max}}$ = extinction coefficient of the specie HInd at the wavelength λ_{HInd}^{max}

$$\dagger e_1 = \epsilon_{HInd-}^{\lambda_{HInd-}^{max}} / \epsilon_{HInd}^{\lambda_{HInd}^{max}}$$

$$\ddagger e_2 = \epsilon_{Ind-}^{\lambda_{Ind-}^{max}} / \epsilon_{HInd}^{\lambda_{HInd}^{max}}$$

$$\P e_3 = \epsilon_{Ind-}^{\lambda_{Ind-}^{max}} / \epsilon_{HInd}^{\lambda_{HInd}^{max}}$$

||Meta-cresol purple (Clayton and Byrne 1993)

#Thymol blue (Zhang and Byrne 1996)

**Phenol red (Robert-Baldo et al. 1985)

(Robert-Baldo et al. 1985), meta-cresol purple (Clayton and Byrne 1993), and thymol blue (Zhang and Byrne 1996) (Table 2).

The indicator dye calibrations of meta-cresol purple (Clayton and Byrne 1993) and thymol blue (Zhang and Byrne 1996) have been made with Tris/TrisH⁺-buffers according to Dickson (Dickson 1993b). The published accuracy for this Tris/TrisH⁺-buffer equation is ± 0.002 pH units. However DelValls and Dickson (1998) have corrected these buffer equations for a general pH offset of $+0.0047$ units, which has to be (and was) added to all seawater measurements.

The general pH calculation procedure is given in Eq. 2. In practice, the absorbances used in this equation have to be corrected for light fluctuations, possible pH perturbation resulting from the indicator dye injections, and light scattering by particles. Light fluctuations and scattering have a direct influence on the absorbance. The fluctuation correc-

tions are relatively straightforward, using parallel measurements on a second (slave) channel without a cuvette (Fig. 1). Dispersion due to particles is detected through intensity measurements at a nonabsorbing wavelength of the indicator dye. For example, absorbance calculations for 434 nm (A^{434}) are made as follows:

$$A^{434} = \lg \left(\frac{I_0^{434} \cdot D^{434} \cdot Tr^{695}}{I^{434}} \right) \quad (3)$$

$$= \lg I_0^{434} + \lg D^{434} + \lg Tr^{695} - \lg I^{434}$$

with

$$D^{434} = I^{434(\text{slave})} / I_0^{434(\text{slave})}$$

and

$$Tr^{695} = I^{695} / I_0^{695}$$

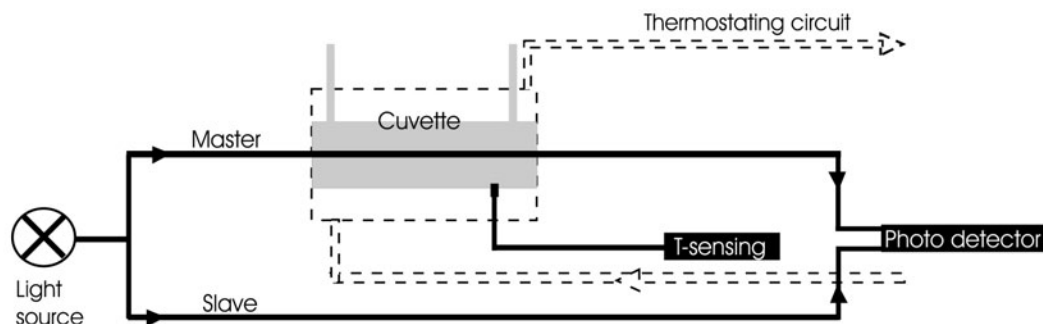


Fig. 1. Schematic overview of the pH system featuring a fiberoptical spectrophotometer with master and slave channel, a thermostating circuit, and a temperature sensor within the cuvette.

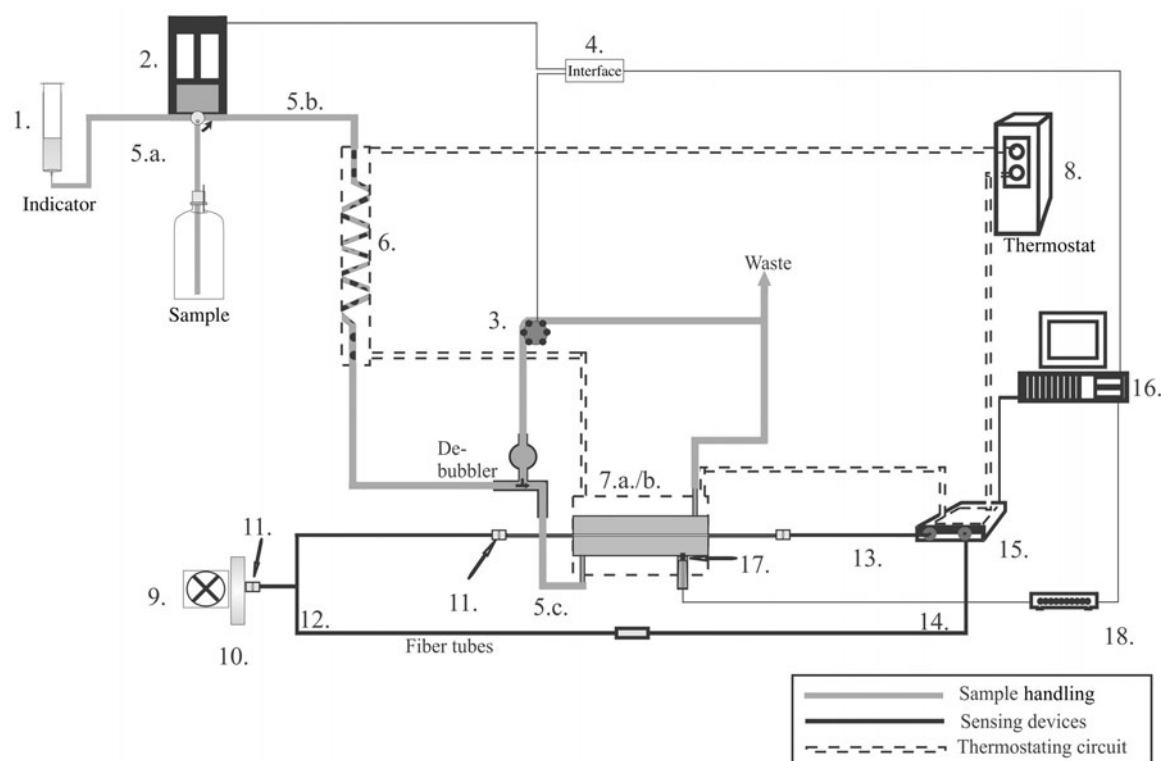


Fig. 2. The discrete spectrophotometric pH system. 1. Control syringe, Luer-Lok and cornwall, 10 mL (Becton Dickinson). 2. Piston pump with 4-way selector valve, model Dosino 700 with dispensing unit 710, 50 mL (Metrohm). 3. Peristaltic pump, model ISM384-0002 (Ismatec SA). 4. Custom-made interface for the Dosino 700 and the peristaltic pump. 5a and 5b. Silicon tube (1/16-inch i.d. and 1/8-inch i.d.), code 10025-02B and 10025-05B (Bio-Chem Valve). 5c. Glass tube (1/8-inch i.d.). 6. Jacketed mixing coil, filled with Pyrex® pearls, model 116-0102-02 (Gradko International). 7a. Quartz-cuvette (100 mm), model QS-165.227 (Hellma GmbH). 7b. Cuvette holder, model CUV-VIS-10 (modified) (Ocean Optics). 8. Refrigerated bath, model F25-MW (Julabo Labortechnik GmbH). 9 to 16. Spectrophotometer unit consisting of (9) tungsten lamp (short life bulb), model HL-2000-FHSA (Mikropack GmbH), (10) filter glass combination of 1-mm BG 24a/1-mm KG 3/1-mm BG 40 (Schott Glas), (11) collimator lenses, model 74-VIS, (12) bifurcated UV/VIS fiber bundle $40 \times 50 \mu\text{m}$ with a 8- to 32-fiber splitting, (13) UV/VIS-fiber bundle $25 \times 50 \mu\text{m}$, (14) UV/VIS-fiber $50 \mu\text{m}$, (15) a two-channel CCD detector modified with a cooling unit, model SD2000, (16) IBM PC with A/D-converter (spectrophotometer module) and IEEE-card (T-sensing); A/D-card, model AD500 (Ocean Optics). 17. 4-wire platinum resistance probe (100 Ω) built in a titanium cap, model S245PD12/AC887 \times 28L36 (Minco Product). 18. Digital multimeter, model DMM 6001 (Prema Präzisions elektronik GmbH).

whereby I is the light intensity, D is a factor compensating for light fluctuations, and Tr is the transparency (the dispersion correction). Index $_0$ stands for the reference measurements at the time when the sample is measured using no indicator. The superscripts indicate the wavelength. Our choice to use a wavelength of 695 nm for the transparency correction, instead of the usually proposed 730 nm, is due to the light spectrum provided (see p 144).

After these corrections, the calculated absorbance ratio should be corrected for the effect of the indicator dye injection, because this injection adds another acid base system to the sample. An exact indicator dye concentration is determined from the absorbance at the isosbestic wavelength of the indicator. The absorbance at this point is dependent only on the total indicator concentration because the extinction coefficients of the protonated and the unprotonated form are equal at this wavelength. Several different methods have been proposed for indicator dye correction (Chierici et al. 1999; Clayton

and Byrne 1993; Hunter and Macaskill 1999). Following the recommendation of Clayton and Byrne (1993), we measured each sample twice, first with an indicator injection of 75 μL and then with a 150- μL injection. Afterwards we measured the additional perturbation and corrected the pH measurements to the 0 μL indicator case.

System and automated sample handling—An overview of the fully automated discrete pH system is given in Fig. 2. The system is a bench-top system and consists of three independent units: sample handling system, thermostating circuit, and sensing devices. A system description is given along these units. All numbers below refer to the numbers appearing in Fig. 2.

The sample handling system ensures thorough mixing, precise sample/indicator volume ratios, and sharp sample separation. Mixing of sample and indicator is achieved through a piston pump that includes a planar 4-way selector valve (2). Small indicator dye injections of 75 μL per 50 mL of sample occur within a loading cycle and result in a nearly homoge-

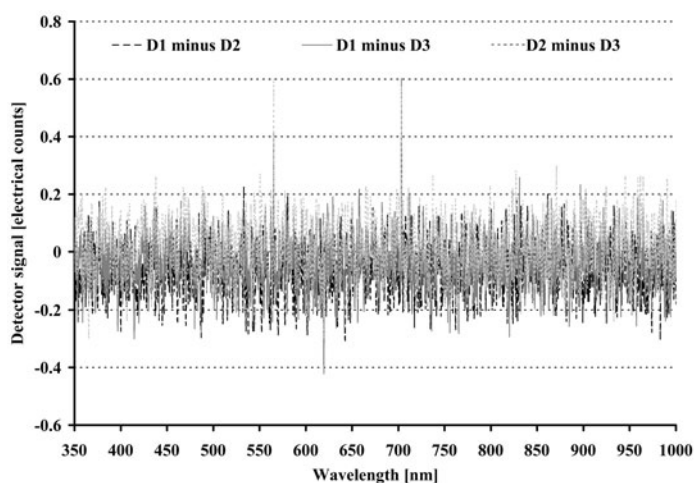


Fig. 3. Averaged spectrophotometer noise (model: SD2000, see Fig. 2) from three dark spectra (D1, D2, D3), the settings were 1000 scans to average, 30 ms per scan, and a constant temperature of 22°C. The CCD spectrophotometer consists of 2048 photosensitive pixels, which cover a bandwidth of 350 to 1000 nm at each channel. For a 3 σ -confidence interval the signal noise is ± 0.25 electrical counts.

nous mixing due to stepwise loading of 975 μL sample followed by 75 μL (150 μL) indicator and 49 mL sample at high velocity of the piston pump. Indicator inhomogeneities that still occur within the sample/indicator mixture are eliminated when the sample stream passes through the thermostated, bead-filled mixing coil (6). Because of sample warming, degassing from the sample can occur at the tube surfaces. In the closed-stream system, spontaneously formed bubbles have an insignificant effect on the pH due to CO_2 exchange. However, they do have a strong optical impact and therefore have to be removed before they enter the cuvette. The corresponding debubbler (for detail, see Fig. 2) is a T-connector with a 2-mL spherical dome at the top. The dome's end is connected to a peristaltic pump (3), which is activated when a sample is filled into the cuvette. Small bubbles are collected in the dome and removed by the peristaltic pump. With this debubbler unit, the total loss of sample/indicator mixture for an entire stroke is ~ 1 mL (out of 50 mL).

A clear sample separation is achieved by a turbulent sample flow through the system, which is supported by small-tube diameters (5a,b,c) and high flow rates (0.8 mL s^{-1}). Additionally, the dead space is minimized by the dead space free piston pump and short connections between the different system components. The 50-mL throw of the piston pump passes through total internal volumes of 4 mL for all tubing, 1 mL for the debubbler system, and 5 mL for the cuvette (7). Photometric testing showed an exchange rate of 99% per full piston stroke. The testing was done by injection of high mCP indicator dye concentrations into the system and observation of isobestic point (488 nm) absorbance after injection of seawater

that contained no indicator. Hence the measurement routine requires one piston stroke for purging, a second one for pure sample loading (taking the reference spectra without indicator, I_0), and a third one for sample/indicator loading (taking the indicator spectra, I).

The sensing devices include a two-channel CCD spectrophotometer (15,16) with tungsten lamp (9), filters (10), collimator lenses (11), optical fibers (12), and a multimeter for temperature measurement (18) using a 4-wire Pt-100 platinum resistance probe (17).

Thermostating maintains a constant temperature of the optical benches in the CCD detector and also of the sample. The latter is achieved with a jacketed mixing coil where a large surface promotes heat exchange. Constant temperatures during measurement are ensured by a water jacket surrounding the cuvette.

All testing was done with 2 mmol L^{-1} meta-cresol purple sodium salt ($\sim 90\%$ dye content, Aldrich Chem.) dissolved in seawater (Certified Reference Materials [CRM] 45; Dickson 1990) that was poisoned with mercuric chloride. The final indicator concentration in the cuvette was 3 and 6 $\mu\text{mol L}^{-1}$ for injections of 75 and 150 μL indicator stock solution, respectively.

CCD detector—The principal element of a CCD detector is a photosensitive semiconductor array with electronic control and A/D-converter. We used a two-channel detector, which features arrays with 2048 pixels, gratings for vis/color-spectra, and 100 μm slits. The optical pixel resolution is 0.33 nm/pixel. Hardware properties were evaluated and compared to the spectrophotometric pH literature.

Theoretical considerations for the required sensitivity of ± 0.001 pH units led to some additional improvements for signal processing, including the A/D-conversion and the signal-to-noise ratio of the detector. The A/D-card converts to 12-bit signals, which are 4096 ($= 2^{12}$) levels in integers. Although mantissas were calculated through signal averaging from 1000 spectra, we found a signal noise of ± 0.25 counts (Fig. 3). This noise level is calculated from the confidence interval of 3 σ for dark and indicator spectra. The conversion of this noise level into absorbance units depends on the total light attenuation, as shown in Fig. 4. There we calculated the errors in absorbance (δA) as a function of the intensity (I). δA has a direct influence on the pH according to Eq. 2, where for meta-cresol purple R is A^{578}/A^{434} . For larger R ratios, the e -terms in Eq. 2 become small or constant and the pH can be roughly estimated by:

$$\text{pH}_x = \text{pK}_{\text{ind}} + \lg \frac{A^{578}}{A^{434}} - \lg(\text{const.}) \quad (4)$$

Hence the error in pH depends on the absorbance ratio.

In the extreme case, an R value of 3.006 instead of the true 3.000 yields an error in pH of -0.001 . So a deviation of ± 0.002 absorbance units for intensities down to 109 counts seems to be acceptable with regard to the resulting error in pH.

In addition to theoretical aspects, we compared our spectrophotometer configurations to the calibrations of meta-cresol purple (Clayton and Byrne 1993) and thymol blue (Zhang and

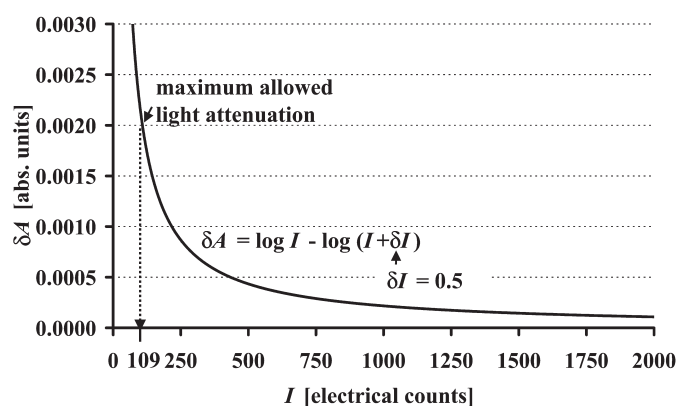


Fig. 4. Assessment of the CCD spectrophotometer capability for accurate pH measurements. We checked the maximum allowed light attenuation for a noise level of 0.5 electrical counts (δI), i.e., the two times 3σ -confidence interval considering dark and indicator spectra. We calculated the errors in absorbance (δA) as a function of the intensity (I). δA has a direct influence on the pH according to Eq. 2 and 4. For a pH of ~ 8.3 R becomes 3.000, and so the light attenuation should not be below 109 electrical counts (see text).

Byrne 1996). Byrne and coworkers used the Cary 1, Cary 3, and Cary 17D (formerly Cary 400, including small changes) double-beam spectrophotometers (Varian). The Varian® instruments have a wavelength accuracy of ± 0.1 nm, single (Cary 1) or double monochromator units, and a spectral bandwidth setting of 1 nm for the calibration (Byrne and Zhang pers. comm. unref.). The monochromator unit of the OceanOptics spectrophotometer SD2000 is a vis/color diffraction grating and 50 μm optical fiber that works as a diffraction slit additionally. The SD2000 has a wavelength accuracy of ± 0.15 nm and flexible bandwidths settings of $n \times 0.33$ nm (n = number of pixels). Hence for $n = 3$, we are in good agreement with the system used by Byrne and coworkers (Clayton and Byrne 1993; Zhang and Byrne 1996; Byrne and Zhang pers. comm. unref.).

Light source, optical filters, and fiber optics—The light source should have an intense spectrum that is as close as possible to an ideal rectangular signal and constant intensities with time. For measurements using only one indicator dye, a spectrum of high intensities at its absorbance maximum, isobestic point, and a nonabsorbing wavelength would suffice. Overall a light spectrum, with high intensities for the whole necessary wavelength range, would allow measurements that are not limited by the light source. Unfortunately there is no light source available with such specifications. In practice, it is a problem to find a light source with adequate intensities near 430 nm, which is required for all spectrophotometric pH determinations made to date. The emitted raw spectrum and the ideal spectrum are being compared in Fig. 5. There are huge differences between these spectra at smaller wavelengths showing that a tungsten lamp cannot provide the minimum requirement of 109 electrical counts at the detector as explained above. Accordingly we modified the relative light intensities at 434 nm using opti-

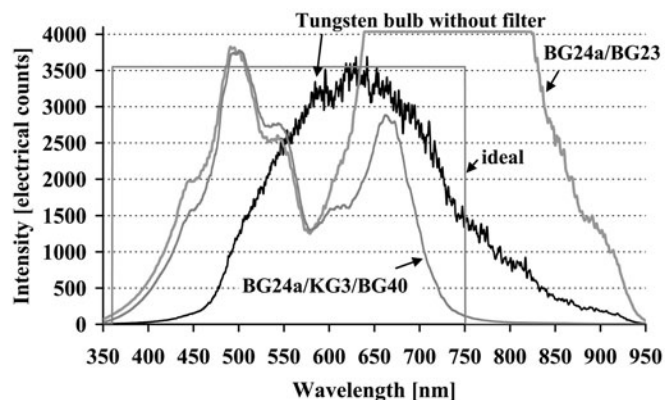


Fig. 5. Detector signals of a tungsten lamp (2960 K) with and without filter combinations as well as the ideal rectangle signal. All filtered signals are smoothed. Each filter used in the filter combinations is 1-mm thick and obtained from Schott Glas.

cal filters as shown in Fig. 5. Experiments with seawater as medium in the 10 cm cuvette led to use of a filter combination consisting of Schott® glass BG 24a/KG 3/BG 40 with a thickness of 1 mm each. The filters provided about the same light intensity at all wavelengths of interest. The resulting general light dampening was compensated by use of longer scanning times and the use of fiber bundles. The fiber bundle from the light source consisted of 40×50 - μm -fibers with 32/8 splitting for master/slave channel respectively (12). All fibers were fixed in rubber foam because of the significant variations in light attenuation that can occur due to fiber bending.

Influence of wavelength bandwidth—Indicator dye calibrations as described in the literature have been performed using expensive, high accuracy scanning spectrophotometers with photo multipliers. These photometers are capable of making absorbance measurements with variable wavelength bandwidth from 0.1 to 5 nm. In cheaper spectrophotometers with CCD or PDA detectors, the choice of this bandwidth is limited by the number of pixels/diodes per nanometer. For example, DelValls (1999) used a PDA spectrophotometer with a bandwidth of 2.5 nm per pixel. Although the deprotonated and protonated indicator form both have broad absorption bands, the decrease of the extinction coefficients as a function of wavelength is not symmetrical left and right of the absorbance-maximums.

We tested the influence of optical pixel resolution of the CCD detector on our pH calculations using measurements on 75 samples (Fig. 6). The sample pH was first measured in the standard configuration with a 1-nm bandwidth as a reference. Subsequent calculations with bandwidth of 0.33, 1.67, and 2.33 nm are expressed in pH deviations from this reference. Mean deviations ($\pm 1s$) of 0.00018 ± 0.00037 , 0.00002 ± 0.00017 , and 0.00002 ± 0.00024 , respectively, indicate that the deviations are random and originate from detector noise. Smaller bandwidths are much more susceptible to noise, although a deviation of 0.00018 ± 0.00037 pH units for the 0.33 nm and

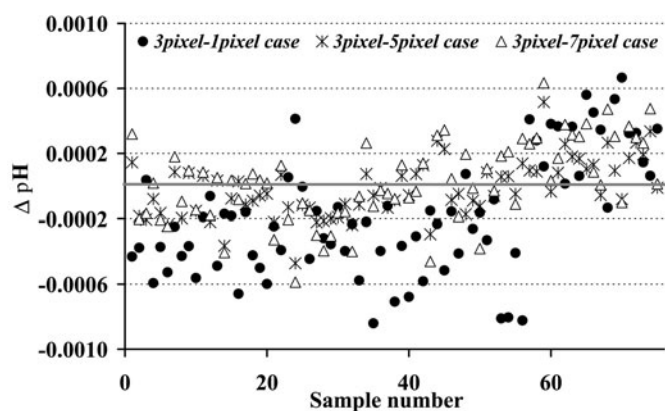


Fig. 6. Plot from 75 pH measurements with pH_T ranging from 7.750 to 8.000. Each sample pH has been calculated four times using the same optical spectra but different optical resolution/bandwidth of one, three, five, seven pixels at the absorbance maxima and control wavelength. The plot shows the pH deviation from the three-pixel-reference (1 nm) case to calculations of one (3pixel-1pixel case), five (3pixel-5pixel case), and seven (3pixel-7pixel case) pixels. Within about two ten-thousand pH-units the bandwidth of three and five pixel case show equivalent results.

1 pixel case seems tolerable. The results indicate that, for this system, the best accuracy is achieved with a bandwidth of 1.67 nm for which minimal errors from extinction coefficient changes and detector noise are encountered.

Temperature measurement—High accuracy pH measurements depend strongly on reliable temperature measurements. A temperature uncertainty of ± 0.03 K leads to uncertainties in the pH of ± 0.001 pH units for Tris/TrisH⁺-buffers. Therefore we carefully calibrated our 4-wire Pt-100 platinum resistance probe against a F250 device (Automatic Systems Laboratories) using a calibrated 4-wire platinum resistance thermometer (type nr: T25/02, serial nr: A/68) with a NAMAS certified accuracy of ± 0.01 K. After a simple offset correction the accuracy of the temperature measurement was better than ± 0.03 K. This accuracy was checked for stability over a 6-month interval.

Options, settings, and raw data storage—The automated pH system (Fig. 2) provides several options for sample/data processing and for hardware testing. Processing options allow the use of three different indicators (Table 2), variable mixing ratios from 1/1000 (sample/indicator), as well as flexibility in the choice of scanning times and the number of scans to average. A repeat mode provides convenient replicate measurements on larger seawater sample reservoirs.

A second-order polynomial of wavelength versus pixel can be derived (or verified) for master and slave channel by an auto calibration function. For this option the system configuration has to be modified with a mercury-argon lamp (model HG-1, Ocean Optics Inc.) as a light source with a discrete wavelength spectrum and has to be connected directly with an 8- μ m fiber to the corresponding detector channel. For the spectrophotometer setup, the manufacturer's (Ocean Optics

Inc.) mercury-argon lamp calibration was used.

Optimal system settings, which resulted from testing of the spectrophotometric subunit, are scanning times from 17 to 56 ms, averaging of detector signals of 1000 scans, optical bandwidths of 1.67 nm ($n = 5$) for the three relevant indicator wavelengths, and 3.33 nm ($n = 10$) for the transparency at 695 nm. These settings resulted in maximum detector signals of ~ 1350 electrical counts at 430, 580, and 695 nm and ~ 3200 electrical counts at 490 nm. Regarding the detector noise of ± 0.25 electrical counts at 1000 scans to average (Fig. 3), the suitable operating range is up to not more than 1 absorbance unit at each wavelength.

During measurements all system settings (e.g., scanning time, sample salinity input, indicator equation coefficients, detector calibration polynomial, and so on) and all raw data such as dark spectra, reference spectra, indicator spectra, and measurement temperature (normally 22°C) are saved. On this basis recalculation can be performed afterward using a separate program.

Analytical precautions—All samples were collected according to a standard technique for dissolved gases described by the U.S. Department of Energy (1994). Surface-to-deep water samples (10 to 4800 m) were taken from hydrocasts.

For best results, samples were thermostated within the system bath (Fig. 2) for about 8 min near to 22°C, which is close to the final sample temperature of the thermostated cuvette. To avoid spectral disturbances of the samples due to degassing after the debubbler system, each tube and the cuvette was soaked in water for at least 24 h and then built into the system as fast as possible. The light source had to be configured with a short-life bulb (operating temperature 2960 K) because of the more favorable emission spectrum. In comparison to the spectrum of the long-life bulb (operating temperature 2800 K) the 'short-life spectrum' had much higher light intensities, especially at 430 nm. The CCD detector with wire and PC was built in a grounded Faraday cage. By this measure, undefined signal disturbances were eliminated. The shielding was made from aluminum foil.

Assessment and discussion

System precision—The system was evaluated with respect to its long- and short-term precision. Long-term precision was assessed from multiple measurements of individually bottled Certified Reference Materials (Dickson 1990) during the North Atlantic Meteor cruise M45-2 and -3 (Fig. 7). Short-term precision was estimated from repeated measurements on a single container of seawater.

Determining precision by testing that is based on CRM instead of the Tris/TrisH⁺-buffer alternative includes the great advantage of also allowing direct comparisons with measurements of other inorganic carbon parameters, including measurements made at other times and in other laboratories using different techniques. This is particularly important for discrete measurements of pH because, to date, relatively few at-sea measurement campaigns have included measurements of this parameter. TCO₂ and TA

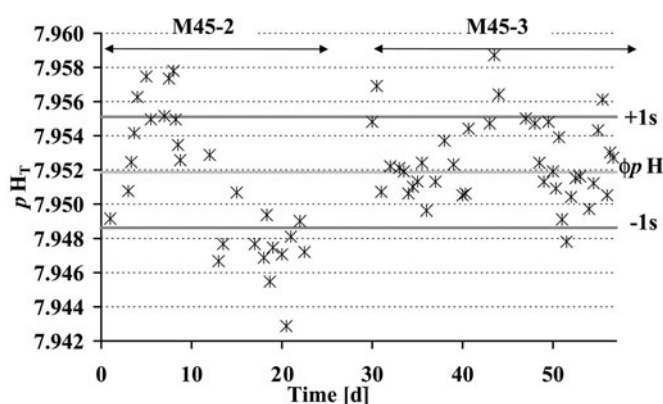


Fig. 7. Long-term precision based on repeated measurements on individual bottles of CRM batch nr 45 during the Meteor cruise 45-2 and -3 from June-August (indicator dye correction after Clayton and Byrne [1993], calibration correction after DelValls and Dickson [1998]). The calculated standard deviation is ± 0.0032 for 67 CRM analyses.

have until now been more commonly measured. Measurement of CRM, which are well characterized in terms of TCO_2 and TA, offers a means to compare pH measurements.

The system's long-term pH precision from 67 CRM, analyzed over a period of 2 months, was ± 0.0032 (1s). This is equivalent to a precision of ± 1.1 to $2.2 \mu\text{mol kg}^{-1}$ in TCO_2 and ± 1.4 to $2.1 \mu\text{mol kg}^{-1}$ in TA, depending on temperature and the TCO_2/TA ratio. This level of precision is comparable to the precision of TCO_2 and TA achieved in state-of-the-art field measurements made during the U.S. Indian Ocean CO_2 Survey 1994-1996 (Johnson et al. 1998; Millero et al. 1998). These showed typical TCO_2 precisions of 0.79 to $1.88 \mu\text{mol kg}^{-1}$ and typical TA precisions of 1.4 to $5.1 \mu\text{mol kg}^{-1}$ for sub-sample sets, i.e., cruise legs that were controlled for quality by a total number of 31 to 101 CRM measurements.

A more detailed look at Fig. 7 shows a smaller scatter around the mean from the second to the third cruise leg from ± 0.0042 (1s) to ± 0.0022 (1s). We suppose this was caused by too infrequent zero compensations of the temperature measurement device with the 4-wire platinum resistance probe (Fig. 2). This was changed to a daily compensation on the third leg. Because this was the only change, it is likely that the better overall performance is due to a more accurate and precise temperature measurement.

The mean pH_T at 22°C from all measurements of CRM nr 45 was 7.9519. This is within -0.0016 pH units of the pH_T value calculated from certified values of TCO_2 and TA (salinity = 33.487, $\text{TCO}_2 = 1994.17$, TA = 2204.4) using the program CO2SYS (Lewis and Wallace 1998) with the constants of Mehrbach et al. (1973) after the refit of Dickson and Millero (1987). Dickson and coworkers (pers. comm. unref.; Scripps Institution of Oceanography) found comparably good agreements between spectrophotometrically measured and calculated pH_T values from CRM batch nrs 59, 60, and 61 using certified values and the constants of Mehrbach et al. (1973) from

a more recent refit by Lueker et al. (2000). In contrast to our findings, their measurements were by a mean of 0.003 pH units higher than the calculated.

Short-term precision was determined by multiple replicate measurements made on 6 L of mercury-chloride-poisoned Baltic Sea seawater, which was stored in a closed, flexible, and gas-impermeable plastic bag without headspace. The standard deviation of 29 replicate measurements gave a short-term precision of 0.0012 pH-units (1s). We made no correction for the small temperature variations (23.13°C to 23.19°C) within the cuvette, as we could not find a significant correlation between temperature and pH change. This finding is in agreement with the statements of Byrne and Breland (1989) and Clayton and Byrne (1993), who found that spectrophotometric pH determinations with sulfonephthalein indicators are rather insensitive to such temperature fluctuations, because the temperature dependency of the dissociation constants of indicator and CO_2 -system are similar. Previously published at-sea (1s) precision estimates for batch measurements vary from 0.0004 (photomultiplier-based) (Clayton and Byrne 1993) to 0.005 (PDA) (Bellerby et al. 1995) pH units. Based on our estimate of short-term precision, our pH technique (CCD) is of comparable quality to state-of-the-art TCO_2 - and TA-analyses.

System accuracy—We assessed the system accuracy using a Tris/TrisH⁺-seawater buffer prepared according to Dickson (1993b), because this buffer was the basis of the thymol blue and meta-cresol purple calibration of Byrne and coworkers (Zhang and Byrne 1996; Clayton and Byrne 1993). The Tris buffer substance with a mass fraction of $99.901\% \pm 0.021\%$ was obtained from the NIST (National Institute of Standards and Technology, Gaithersburg, MD, USA). After buffer preparation, we filled seven 500-mL Pyrex bottles following the standard procedure of CO_2 sampling (DOE 1994), but sampling the pure buffer from the 10 L container of preparation. We planned to determine the pH_T of each bottle over 7 weeks, i.e., one bottle per week. The first two pH_T -measurements of bottle 1 were done directly after the seawater buffer preparation and had satisfying results, with slightly too high pH_T measurements of 0.0012 at 22°C . The two measurements were, within the estimated precision of ± 0.0012 , in perfect agreement with the calculated values after Clayton and Byrne (1993). Consistently, we did not correct these pH_T measurements according to DelValls and Dickson (1998), because Clayton and Byrne's calibration was done without such information. Unfavorably, the planned series of buffer measurements was not feasible because we had not included antibiotics and found mold in all stored buffer bottles later on. Therefore only the first two measurements were used.

Overall pH accuracy or the true seawater pH—In terms of a direct comparability of our pH to another CO_2 parameter the question is: "How near is our pH measurement to the true pH value?"; i.e., how do fundamental assumptions, buffer calibrations, dye calibrations, and our measurement accuracy work into the pH accuracy? So the overall assessment of pH accu-

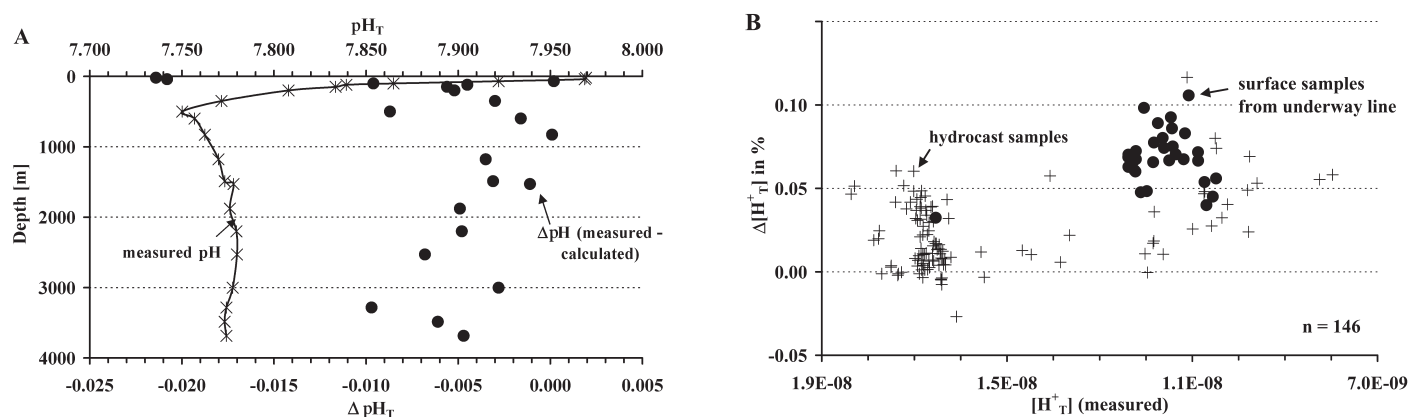


Fig. 8. Thermodynamic pH_T consistency check (at 22°C) from TCO_2 and TA data for 112 Niskin bottles and 34 discrete upper surface samples (4 m) from an underway water supply using the constants of Mehrbach et al. (1973) (indicator dye correction after Clayton and Byrne [1993], indicator calibration correction after DeValls and Dickson [1998]). A measured surface-to-deep water pH_T -profile at *Transient Tracers in the Ocean* location 121 (52.645°N 27.008°W) and residuals from $\text{pH}_T(\text{measured}) - \text{pH}_T(\text{calculated})$; ($n = 21$). B Plot of $\Delta[\text{H}^+]_T$ in % = $[\text{H}_T(\text{measured}) - \text{H}_T(\text{calculated})]/\text{H}_T(\text{measured})$ versus $[\text{H}^+]_T$ (measured) according to McElligott et al. (1998); ($n = 146$).

curacy has to acknowledge (1) the thermodynamic assumptions made by seawater buffer introduction, (2) the accuracy of the buffer calibration, (3) the accuracy loss in the determination of the spectrophotometric indicator dye equation itself, and (4) the measurement accuracy of our determining system.

According to Dickson (1993b), the thermodynamic model used for seawater buffer calibrations neglects differences between the activity coefficients of free- and base-associated hydrogen ion. This causes a non-random uncertainty of less than 0.004 pH units. The procedure for the buffer calibration itself has a random error of ± 0.002 pH units based on residuals of measured minus calculated pH values. In this context, it is worth noting that in several cases only this latter uncertainty of ± 0.002 pH units is described as accuracy (DOE 1994; Lee and Millero 1995; Chierici et al. 1999). The indicator calibrations of Clayton and Byrne (1993) and Zhang and Byrne (1996) have additional uncertainties of ± 0.001 pH units. Our system accuracy estimate from the CRM measurements was of ± 0.0032 pH units. Combining the last three random uncertainties (by the square root of the sum of squares of each accuracy) leads to a true accuracy in our pH determination of ± 0.004 pH units plus a possible systematic error of ± 0.004 pH from the introduction of the hydrogen ion seawater scales.

Thermodynamic internal consistency—An alternative means of assessing system accuracy is to evaluate the internal consistency between parallel measurements of CO_2 system parameters made on the same samples. Internal thermodynamic consistency is the degree to which the independent measures of an overdetermined CO_2 system agree with each other. Although there are, inevitably, uncertainties in the apparent dissociation constants used to make such comparisons (Clayton et al. 1995; Lee and Millero 1995; McElligott et al. 1998; Byrne et al. 1999), such a comparison can reveal whether gross errors are being made. Further, the level and nature of internal

consistency can be compared with results of similar comparisons reported by other investigators. This permits us to assess whether similar behavior is observed, and, hence, whether the absolute pH measurements are comparable.

During Meteor cruise M45-2/-3, our pH system was used for measurements on discrete water samples together with nutrient and oxygen analysis and discrete TCO_2 measurements. The latter was performed with the coulometric technique according to Johnson et al. (1993). At several stations, samples were collected and stored for subsequent shore-based measurement of TA to evaluate the thermodynamic consistency of the carbonate system. Storage and analysis for the TA determination was conducted according to DOE (1994). The data quality assessment for TCO_2 and TA analysis was evaluated by CRM measurements and showed (1s) precisions of $\pm 0.62 \mu\text{mol kg}^{-1}$ (TCO_2) and $\pm 1.09 \mu\text{mol kg}^{-1}$ (TA) and mean deviations from the certified values of $-0.32 \mu\text{mol kg}^{-1}$ (TCO_2) and $+0.19 \mu\text{mol kg}^{-1}$ (TA). Thermodynamic calculations were again performed on the total scale by the program CO2SYS (Lewis and Wallace 1998). Detailed information of its calculation procedure—i.e., the pH scale transformation—all dissociation constants used can be found within the program, which is freely available from the FTP server of the Carbon Dioxide Information Analysis Center (<http://cdiac.esd.ornl.gov/oceans/co2rprt.html>). The program choices were made on the usage of the HSO_4^- constant according to Dickson (1993b) and the carbonic acid constants of Mehrbach et al. (1973) as refit by Dickson and Millero (1987). The decision to use the constants of Mehrbach et al. (1973) is based on the good agreement between calculated and measured CRM values (shown above) and also allow comparison with the consistency results of Clayton et al. (1995) and McElligott et al. (1998).

The internal thermodynamic consistency is represented in Fig. 8 for a typical surface-to-deep water profile, and a

[H⁺]-difference plot of 146 samples is shown. The measured surface-to-deep water profile shows, in general, a very good agreement with the (TCO₂/TA) calculated pH profile with differences generally being in the range from 0.000 to -0.025 pH units.

This level of internal consistency suggests that no gross error is being made with our pH measurement. However the magnitude of the averaged difference between measured and calculated pH from the 112 hydro cast samples and 34 surface samples are -0.010 and -0.034, respectively. This therefore exceeds our estimate of the precision and accuracy of our pH measurement by a lot. The difference may result from errors in our pH measurement, from errors in the TCO₂ or TA measurements, or alternatively and more likely, the constants used to calculate pH from TA and TCO₂, or all three. The pH error arising from our TCO₂ and TA accuracy is of the order ±0.005 units. Therefore errors in the constants seem the most probable cause. The outlier values of the surface samples in Fig. 8b cannot be explained easily but could be due to the sampling technique that may provide inexact salinity values. A more speculative explanation for the discrepancy could be acid-base systems not reflected in the alkalinity calculation but perhaps present in surface waters. These would directly lead to biases in the calculated carbonate alkalinity and explain why TCO₂ and pH is a better pair to calculate *f*CO₂ compared to the TCO₂ and TA pair reported by McElligott et al. (1998) from 1403 samples. Although this is an interesting interpretation, the focus of Fig. 8 is on the analytical comparability of our pH measurements with earlier pH measurements made with scanning spectrophotometers and photomultipliers.

Our [H⁺]-residual plot can be compared with results from recent independent studies of internal consistency reported by McElligott et al. (1998) and Byrne et al. (1999). Over the pH range of 7.700 to 8.100, our calculated [H⁺] offset of order ~0.03% is consistent with their findings. Hence two recent independent studies using independent pH measurement techniques find a similar level of internal thermodynamic consistency suggesting that the factors underlying the difference between measured and calculated pH may be common (e.g., error in the constants). It is worth noting that their data were obtained with a scanning spectrophotometer instead of the CCD spectrophotometer used in this work. This implies that both types of spectrophotometers can attain similar levels of analytical performance and data quality on field samples.

Comments and conclusions

An automated system for the measurement of seawater pH has been developed, tested, and fully described, including a technical evaluation of the key factors related to the use of modular CCD spectrophotometers for pH determination. Testing of the light source and the CCD detector clarified the technical requirements for such systems. Notably the white light spectrum emitted from a tungsten lamp has to be modified by optical filters to optimize the light signal for digital signal processing from the CCD detector. In addition, we found that dif-

fering optical bandwidths for absorbance measurements used for the published pH-indicator calibrations and in our new system do not inevitably result in a loss of system accuracy. Hence a larger bandwidth is equal to a higher number of relevant pixels, which results in a smaller signal noise and an improvement in system precision.

The pH method described here is shown to be capable of high-quality measurements comparable to the state-of-the-art measurements of other pH techniques discussed in the literature, as well as other approaches used to determine the inorganic carbon system in seawater. The system is capable of long-term precision of the order ±0.0032 pH units (at sea) and a short-term precision of ±0.0012 pH units. Field data were used to evaluate the method on the basis of the internal thermodynamic consistency of the inorganic carbon system in relation to high-accuracy measurements of TCO₂ and TA. Measured and calculated pH values agreed to within -0.025 and showed behavior consistent with that found in other recent studies concerning internal consistency (McElligott et al. 1998; Byrne et al. 1999). Our results imply that with careful design and testing, inexpensive CCD spectrophotometers can be used for high-accuracy oceanic pH measurement.

References

- Bellerby, R. G. J., A. Olsen, T. Johannessen, P. Croot. 2002. A high precision spectrophotometric method for on-line shipboard seawater pH measurements: the automated marine pH sensor (AMpS). *Talanta* 56(1):61-69.
- , D. R. Turner, G. E. Millward, and P. J. Worsfold. 1995. Shipboard flow injection determination of sea water pH with spectrophotometric detection. *Anal. Chim. Acta.* 309:259-270.
- Buddemeier, R. W., J. -P. Gattuso, and J. A. Kleypas. 1998. Rising CO₂ and marine calcification. *LOICZ Newslet.* 8:1-3.
- Byrne, R. H. 1987. Standardization of standard buffers by visible spectrometry. *Anal. Chem.* 59:1479-1481.
- , and J. A. Breland. 1989. High precision multiwavelength pH determination in seawater using cresol red. *Deep-Sea Res. I* 36(5):803-810.
- , S. McElligott, R. A. Feely, and F. J. Millero. 1999. The role of pH_T measurements in marine CO₂-system characterizations. *Deep-Sea Res.* 46A(11):1985-1997.
- Chierici, M., A. Fransson, and L. G. Anderson. 1999. Influence of m-cresol purple indicator additions on the pH of seawater samples: correction factors evaluated from a chemical speciation model. *Mar. Chem.* 65(3-4):281-290.
- Clayton, T. D., and R. H. Byrne. 1993. Spectrophotometric seawater pH measurements: total hydrogen ion concentration scale calibration of *m*-cresol purple and at-sea results. *Deep-Sea Res.* 40A(10):2115-2129.
- and others. 1995. The role of pH measurements in modern oceanic CO₂-system characterizations: Precision and thermodynamic consistency. *Deep-Sea Res.* 42B(2-3): 411-429.

- Culberson, C., R. M. Pytkowicz, and J. E. Hawley. 1970. Sea-water alkalinity determination by the pH method. *J. Mar. Res.* 28(1):15-21.
- DelValls, T. A. 1999. Underway pH measurement in upwelling conditions: the California Current. *Ciencias Marinas* 25(3):345-365.
- , and A. G. Dickson. 1998. The pH of buffers based on 2-amino-2-hydroxymethyl-1,3-propanediol ('tris') in synthetic sea water. *Deep-Sea Res.* 49A(9):1793-1808.
- Dickson, A. G. 1990. The oceanic carbon dioxide system: planning for quality data, p. 2., JGOFS News, Vol. 2.
- . 1993a. The measurement of seawater pH. *Mar. Chem.* 44(2-4):131-142.
- . 1993b. pH buffers for sea water media based on the total hydrogen ion concentration scale. *Deep-Sea Res.* 40A(1):107-118.
- and F. J. Millero. 1987. A comparison of the equilibrium constants for the dissociation of carbonic acid in seawater media. *Deep-Sea Res.* 34A(10):1733-1743.
- DOE (U.S. Department of Energy). 1994. Handbook of methods for the analysis of various parameters of the carbon dioxide system in sea water. In A. G. Dickson and C. Goyet [eds.], Version 2.0 U. S. Dept. of Energy, Oak Ridge Natl. Lab.
- Hunter, K. A., and B. Macaskill. 1999. Temperature and dye corrections in the spectrophotometric measurement of pH in surface seawater. 2nd International Symposium CO₂ in the Oceans, p 471-479.
- Johnson, K. M., and others. 1998. Coulometric total carbon dioxide analysis for marine studies: assessment of the quality of total inorganic carbon measurements made during the U.S. Indian Ocean CO₂ Survey 1994–1996. *Mar. Chem.* 63(1-2):21-37.
- , K. D. Wills, D. B. Butler, W. K. Johnson, and C. S. Wong. 1993. Coulometric total carbon dioxide analysis for marine studies: Maximizing the performance of an automated gas extraction system and coulometric detector. *Mar. Chem.* 44(2-4):167–188.
- Lee, K., and F. J. Millero. 1995. Thermodynamic studies of the carbonate system in seawater. *Deep-Sea Res.* 42A(11–12): 2035-2061.
- Lewis, E., and D. W. R. Wallace. 1998. CO₂SYS—Program developed for the CO₂ system calculations. Carbon Dioxide Inf. Anal. Center; Report ORNL/CDIAC-105.
- Lueker, T. J., A. G. Dickson, and C. D. Keeling. 2000. Ocean *p*CO₂ calculated from dissolved inorganic carbon, alkalinity, and equations for *K*₁ and *K*₂: validation-based on laboratory measurements of CO₂ in gas and seawater at equilibrium. *Mar. Chem.* 70(1-3):105–119.
- McElligott, S., R. H. Byrne, K. Lee, R. Wanninkhof, F. J. Millero, and R. A. Feely. 1998. Discrete water column measurements of CO₂ fugacity and pH_T in seawater: a comparison of direct measurements and thermodynamic calculations. *Mar. Chem.* 60(1-2):63-73.
- Martz, T. R., J. J. Carr, C. R. French, and M. D. DeGrandpre. 2003. A submersible autonomous sensor for spectrophotometric pH measurements of natural waters. *Anal. Chem.* 75(8):1844–1850.
- Mehrbach, C., C. H. Culberson, J. E. Hawley, and R. M. Pytkowicz. 1973. Measurement of the apparent dissociation constants of carbonic acid in seawater at atmospheric pressure. *Limnol. Oceanogr.* 18:897-907.
- Millero, F. J., and others. 1998. Assessment of the quality of the shipboard measurements of total alkalinity on the WOCE hydrographic program Indian Ocean CO₂ survey cruises 1994–1996. *Mar. Chem.* 63(1-2):9-20.
- Riebesell, U., I. Zondervan, B. Rost, P. D. Tortell, R. E. Zeebe, and F. M. Morel. 2000. Reduced calcification of marine plankton in response to increased atmospheric CO₂. *Nature.* 407:364-367.
- Robert-Baldo, G., M. G. Morris, and R. H. Byrne. 1985. Spectrophotometric determination of seawater pH using phenol red. *Anal. Chem.* 57:2564-2567.
- Tapp, M., K. A. Hunter, K. Currie, and B. Mackaskill. 2000. Apparatus of continuous-flow underway spectrophotometric measurement of surface water pH. *Mar. Chem.* 72(2-4):193-202.
- Wedborg, M., D. R. Turner, L. G. Anderson, and D. Dyrssen. 1999. Determination of pH, p 109-126. In K. Grasshoff, K. Kremling, and M. Erhardt [eds.] *Methods of seawater analysis*, 3rd edition. Wiley-VCH.
- Zhang, H., and R. H. Byrne. 1996. Spectrophotometric pH measurements of surface seawater at in-situ conditions: absorbance and protonation behavior of thymol blue. *Mar. Chem.* 52(1):17-25.

Submitted 10 September 2003

Revised 23 February 2004

Accepted 29 February 2004